Article:

Cen, H, Morina, A and Neville, A (2018) Effect of slide to roll ratio on the micropitting behaviour in rolling-sliding contacts lubricated with ZDDP-containing lubricants. Tribology International, 122. pp. 210-217. ISSN: 0301-679X

https://doi.org/10.1016/j.triboint.2018.02.038

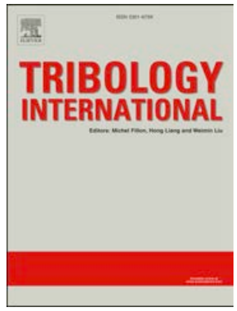

Effect of slide to roll ratio on the micropitting behaviour in rolling-sliding contacts lubricated with ZDDP-containing lubricants

Hui Cen, Ardian Morina, Anne Neville

PII: S0301-679X(18)30125-7
DOI: 10.1016/j.triboint.2018.02.038
Reference: JTRI 5137

To appear in: *Tribology International*

Received Date: 3 January 2018
Revised Date: 21 February 2018
Accepted Date: 24 February 2018

Effect of slide to roll ratio on the micropitting behaviour in rolling-sliding contacts lubricated with ZDDP-containing lubricants

Hui Cen*[a], Ardian Morina*[b], Anne Neville[b]

a- School of Mechano-Electronic Engineering, University of Xuchang, Xuchang, Henan 461000, P.R.China.

b- School of Mechanical Engineering, University of Leeds, United Kingdom.

Abstract

An automated micropitting test rig was applied to study the effect of slide to roll ratio (SRR) on micropitting behaviour in rolling-sliding contacts lubricated with Zinc Dialkyl Dithiophosphate (ZDDP) containing lubricants. The tested specimen surface was examined under an optical microscope and Scanning Electron Microscope(SEM) to study the micropitting behavior of the surface, followed by applying X-ray Photoelectron Spectroscopy(XPS) to study the related tribochemistry behavior. The results show that the increase of SRR can reduce the number of micropits on the worn surface while wear increased and friction did not change much. XPS results indicate that the increase of SRR resulted in the increase of oxide concentration while the decrease of film thickness on the worn surface.

Key words: Slide to roll ratio; Micropitting; ZDDP; Tribochemistry.

*Corresponding author. Tel.: +86 (0)3742968021.

E-mail address: hui.cen@foxmail.com (H. Cen).

a.morina@leeds.ac.uk (A. Morina)

1. Introduction

Micropitting behaviour is a common phenomenon in rolling-sliding tribological systems. There has been a lot of research done on the impact of surface roughness, load, temperature, hardness and slide to roll ratio on micropitting [1-6]. The asperity contact stress between contact surfaces is one of the main reason to promote micropits [1-2]. It is therefore generally considered that micropits can be prevented or lessened by reducing the roughness of the surface or increasing the lambda ratio (through increasing lubricant film thickness or reducing surface roughness). Moreover, Olver and his colleagues [2,6] defined micropitting as rolling contact fatigue caused by roughness. However, the benefit of reducing roughness could be affected by the chemistry of different lubricants [6]. Olver and his colleagues [2,6] found that the micropitting level was lessened by increasing the slide to roll ratio (SRR) but the wear rate did not change significantly.

Additive chemistry has also been proved to affect the micropitting level of the contacting surfaces. Antiwear additives like ZDDP could promote the development of micropits because the additive prevents the removal of the initial roughness of the surface by wear in the running-in period [3-6]. Friction modifiers such as molybdenum dialkyl-dithiocarbamate (MoDTC) can prevent the formation of micropits as a result of the reduction of friction coefficient which then reduces the local tensile stress [7].

Although the effect of SRR and additive chemistry on micropitting has been extensively studied separately, the combined effect of interactions between SRR and additive chemistry on microptting has scarcely been studied. In the current study, the aim is to explore the effect of SRR on micropitting behaviour in the rolling-sliding process when using ZDDP antiwear(AW) additive.

2. Experimental

The tribological tests using two different oils containing ZDDP additive were firstly done in a micropitting rig to study the friction, wear and micropitting performance. The tested specimen after tribological tests was examined by surface analysis technique: an optical microscope and SEM were used to study the micropitting behavior of the surface, and XPS was applied to study the related tribochemistry behaviour on the surface.

2.1 Micopitting rig

The micropitting rig is a three point contact configuration in which three equal diameter discs are pressed into contact with a roller in the centre. This configuration has a high cycle frequency control and a variable slide to roll ratio. The overall appearance of the rig and block view are shown in Fig. 1. The tested lubricants were filled into the chamber with a syringe up to the bottom level of the roller in the centre. Thus, the lubrication between the roller and rings was through the feed of lubricants by the rotation of the two rings at the bottom and the roller. The friction was measured by the strain gauge located on the shaft which is connected to the ring on the top.

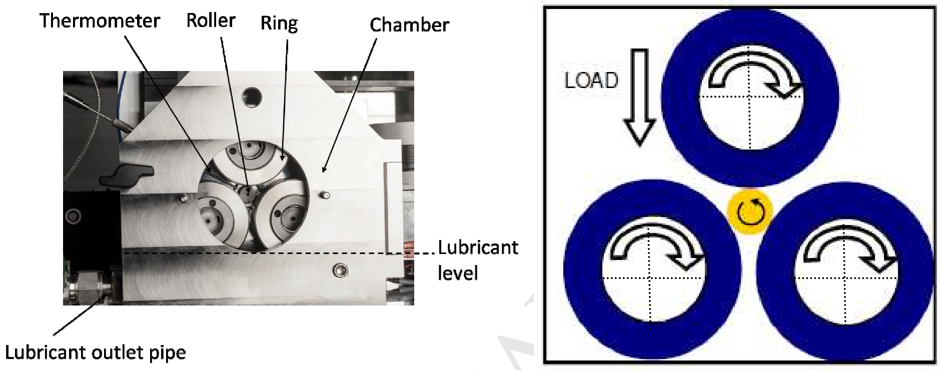

(a) (b)

Fig. 1 Micropitting rig: (a).Overall appearance; (b) Block view.

2.2 Materials and test conditions

The roller used is SRB 21309E from SKF with diameter of 12.05 mm and roughness (*Rq*) less than 50 nm. The ring used is CRB NU 209EC from SKF with outside diameter of 54.45 mm, and 54.15 mm after grinding (transverse to the rotating direction) with average roughness (*Rq*) of 500 nm. Both the roller and ring materials are AISI 52100 steel with hardness 59-66 HRC.

The lubricant used in the micropitting test is composed of base oil PAO, Ester and ZDDP additive (2 *wt%*—the additive mass is 2% of the weight of the lubricant) . Details of the base oil and additive are shown in Table 1. The test conditions are shown in Table 2.

The total test of 720,000 cycles is equal to 2.5 hours. Each test has been repeated three times. The entrainment speed equals to $(V_{roller} + V_{ring})/2$, slide to roll ratio (SRR) equals to $(V_{roller} - V_{ring})/ (V_{roller} + V_{ring})$. Lambda ratio ($\lambda$) is obtained though Eq. 1 where R_{roller} is the average roughness of the roller and R_{ring} is the average roughness of the three rings. The initial contact pressure is calculated from Hertzian initial line contact equation and film thickness, h_{min} is calculated using Eq.2 derived by Dowson and Higginson[8].

$$\lambda = \frac{h_{\min}}{\sqrt{{R_{roller}}^2 + {R_{ring}}^2}} \qquad \textbf{Eq. 1}$$

$$\frac{h_{\min}}{R} = 2.65\{2\alpha E^*\}^{0.54}\left\{\frac{\overline{U}\eta_0}{2E^*R}\right\}^{0.7}\left\{\frac{W}{2E^*RL}\right\}^{-0.13} \qquad \textbf{Eq.2}$$

where λ is the film thickness ratio, h_{min} is minimum film thickness, R is radius of curvature, α is the pressure–viscosity constant, E^* is the equivalent modulus of elasticity, U is the entrainment speed, η_0 is the dynamic viscosity, W is the applied force, and L is contact length (detected by the sensor in the micropitting rig).

Table 1 Details of base oils & additives used

Base Oil & Additive			Kinematic viscosity at 40°*C* (mm^2/s)	Kinematic viscosity at 100°*C* (mm^2/s)	Sulphur content (*wt%*)	Phosphorus content (*wt%*)
Code	Description	Designation				
Synthetic Group IV	Fully synthetic (PAO)	PAO	24.6	5.1	0.00055	<0.00030
Ester additive	Synthetic ester	Ester	26.8	5.5	0.00052	<0.00030
ZDDP additive	Iso-butyl-zinc dithiophosphate	ZDDP	N/A	N/A	23.400	11.300

Table 2 Test conditions

Load (*GPa*)	Temperature (°*C*)	SRR (%)	Entrainment speed (*m/s*)	lambda ratio (λ)	*N*, K Cycles
1.5	75	0.5;2;5	1	0.16	720 (2.5hours)

The friction data acquisition is carried out at a sampling frequency of 1 *Hz* by a strain gauge positioned on the upper disc. The average value of the last 30 minutes in the test is taken as the friction coefficient for the tested lubricant for analysis. Wear volume of the post test roller instead of wear coefficient is used to represent the wear of the roller. To obtain the wear volume on the post test roller, the depth profile on the wear scar is first obtained by Wyko measurement. Wear volume is then calculated through analysing the data of the depth profile. One example of the depth profile obtained by Wyko is shown Fig. 2. The calculation of the wear volume from the depth profile is shown in Eq. 3.

$$V_{wear} = \int \left[\frac{(L_1 + L_2) \times h}{2} \times 2\pi r \right] \qquad \textbf{Eq. 3}$$

Where V_{wear} is the wear volume of the roller; r is the radius of the roller. L_1, L_2 and h are defined in Fig. 2 which shows the dimensions of one element from which the whole integration is performed.

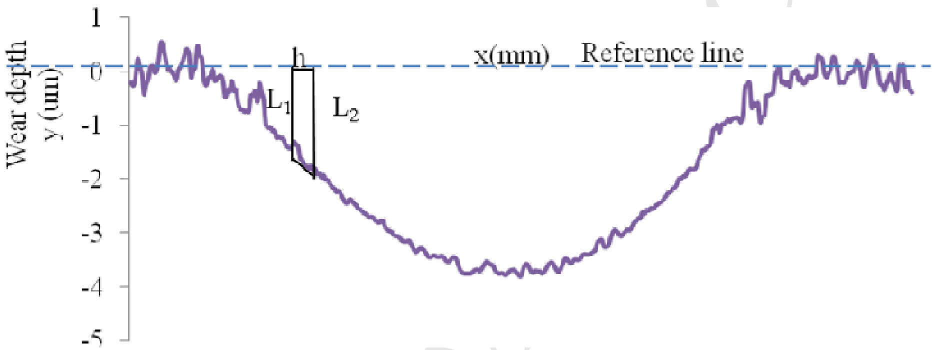

Fig. 2 Sample depth profile on the wear scar of roller after a micropitting test

2.3 Surface analysis techniques

The morphology of the surface film was characterised with Zeiss Supra 55 Scanning Electron Microscope with a 5 kV electron beam voltage in the secondary electron mode.

The X-ray photoelectron spectroscopy measurements were conducted in a PHI 5000 VersaProbe™ X-ray photoelectron spectrometer (Ulvac-PHI Inc, Chanhassen, MN, US) with a monochromatized Al Kα X-ray (1486.6eV) source. In this XPS [9] the emitted electrons are collected and retarded with an Omega lens system at an emission angle of 45°. After passing a spherical capacitor energy analyzer, the electrons are collected by a 16-channel detector. The system is equipped with a high performance floating-column ion gun and an electron neutralizer for charge compensation. The residual pressure was always below 1×10^{-7} Pa.

The identification of the wear track was performed using Scanning X-ray Image (SXI), allowing the visualizing of the desired features on the sample. With regard to the eV resolution of the XPS used, the full width half maximum (fwhm) for $Ag3d_{5/2}$ collected with a power of 4.25 W in the constant-analyzer-energy (CAE) mode, using a pass energy of 58.7 eV and a step size of 0.15 eV was 0.9 eV. Survey spectra and detailed spectra were collected with a beam diameter of 100 μm (only within the wear scar area). Survey spectra were acquired with 117.4 eV pass energy and a step size of 1 eV. Detailed spectra were acquired with 46.95 eV pass energy and a step size of 0.1 eV. The whole set of spectra (detailed and survey spectra) were acquired within 120 minutes. Samples were argon ion sputtered using 2 kV ions over an area of 2×2 mm^2. The same spot size, pass energies and times per step mentioned before for survey and detailed XPS spectra were used during depth profiling acquisition (etching process). XPS data were processed with CASA XPS software (CasaXPS software version 2.3.15 Ltd., UK). The detailed spectra were fitted with Gaussian-Lorentzian curves and a Linear background was used. Before doing curve fitting, all the peaks were calibrated by shifting C 1s to 285.0 eV.

3 Results and discussion

3.1 Tribological results

Friction and wear results under 0.5%, 2% and 5% SRR are shown in Fig. 3. Optical microscope and SEM images of rollers after tribological tests are shown in Fig. 4 and Fig. 5, respectively. The colours observed on the optical microscope images (Fig. 4) are due to the presence of transparent surface films of oxides, and tribofilm traces of lubricant or solvent [7].

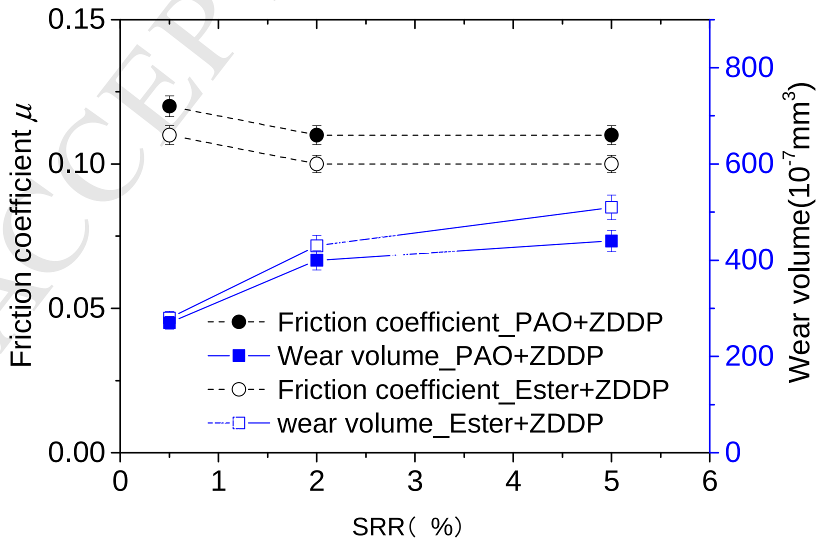

Fig. 3. Tribological results under different SRR

Fig. 3 shows that increasing SRR from 2 to 5% results in increased wear and slight reduction of friction. Ester based oil always showed lower friction but higher wear than those of PAO based oil. The higher wear of Ester based oils could be resulted from the higher polarity of base oil. Suarez *et al.*[10] stated that the polar base oil would compete with ZDDP to attach to the surface hence reduce the adsorption rates of ZDDP which results in higher wear.

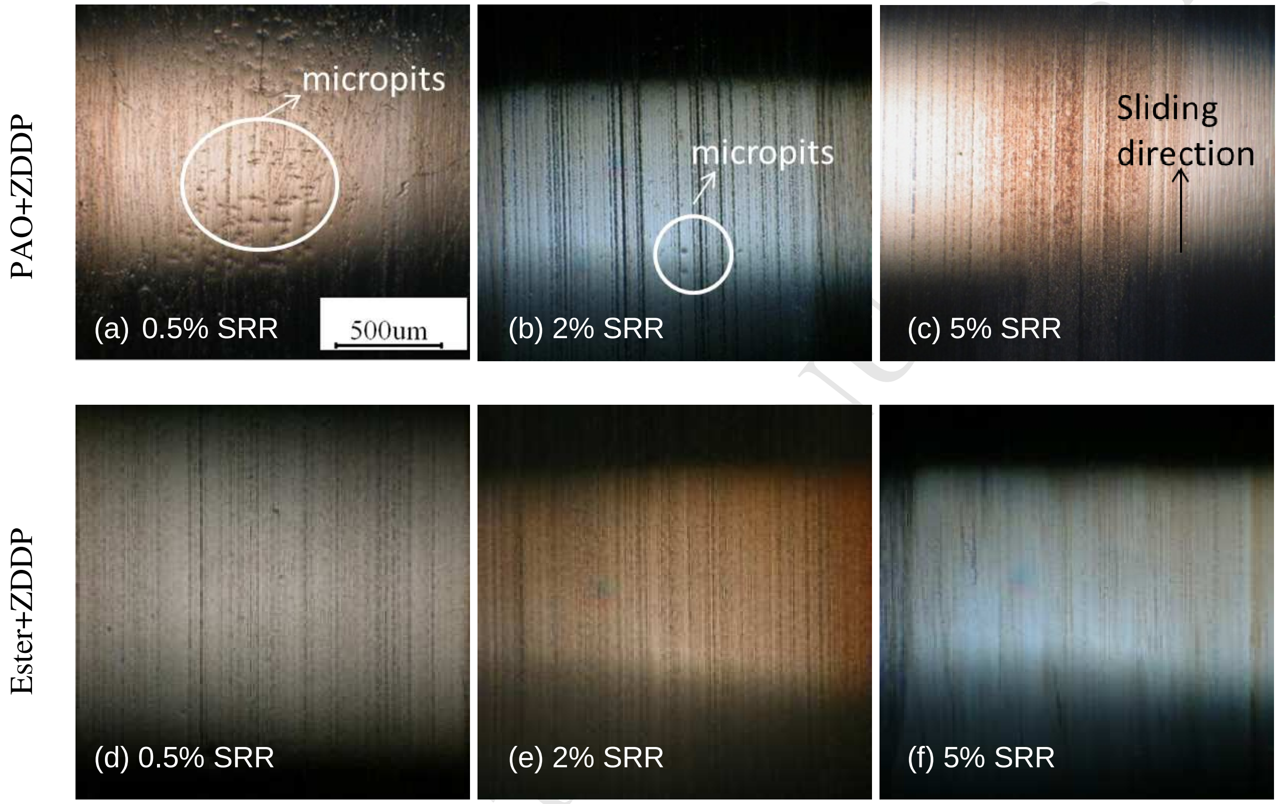

Fig. 4. Optical microscope images of rollers after tribological tests at different SRRs: (a),(b),(c) are for PAO+ZDDP results; (d),(e),(f) are for Ester+ZDDP results; all images are in the same scale as shown in (a).

The optical microscope images shown in Fig. 4 indicate that the number of micropits for PAO+ZDDP oils decreases with SRR, which is also supported by SEM results shown in Fig. 5. On the other hand, there is hardly any micropit shown on roller surface for Ester+ZDDP oils under all tested SRRs. This could be related to the lower friction and higher wear of Ester based oils than PAO oils. Morales-Espejel et al. [11] used the same test rig as in this study and found that the decrease of friction or increase of wear can reduce the micropitting level. Moreover, Lainé *et al.* [7] state that less micropits formed due to the decrease of friction coefficient which is a result of the reduction of the local tensile stress within the contact area. Furthermore, polar Ester base oil can compete with ZDDP additive to attach to the surface which then limits the effect of ZDDP in promoting the formation of micropits as shown in [3-6]. Thus, it not surprising to see that micropits formed when using PAO+ZDDP while hardly any micropit formed when using Ester+ZDDP.

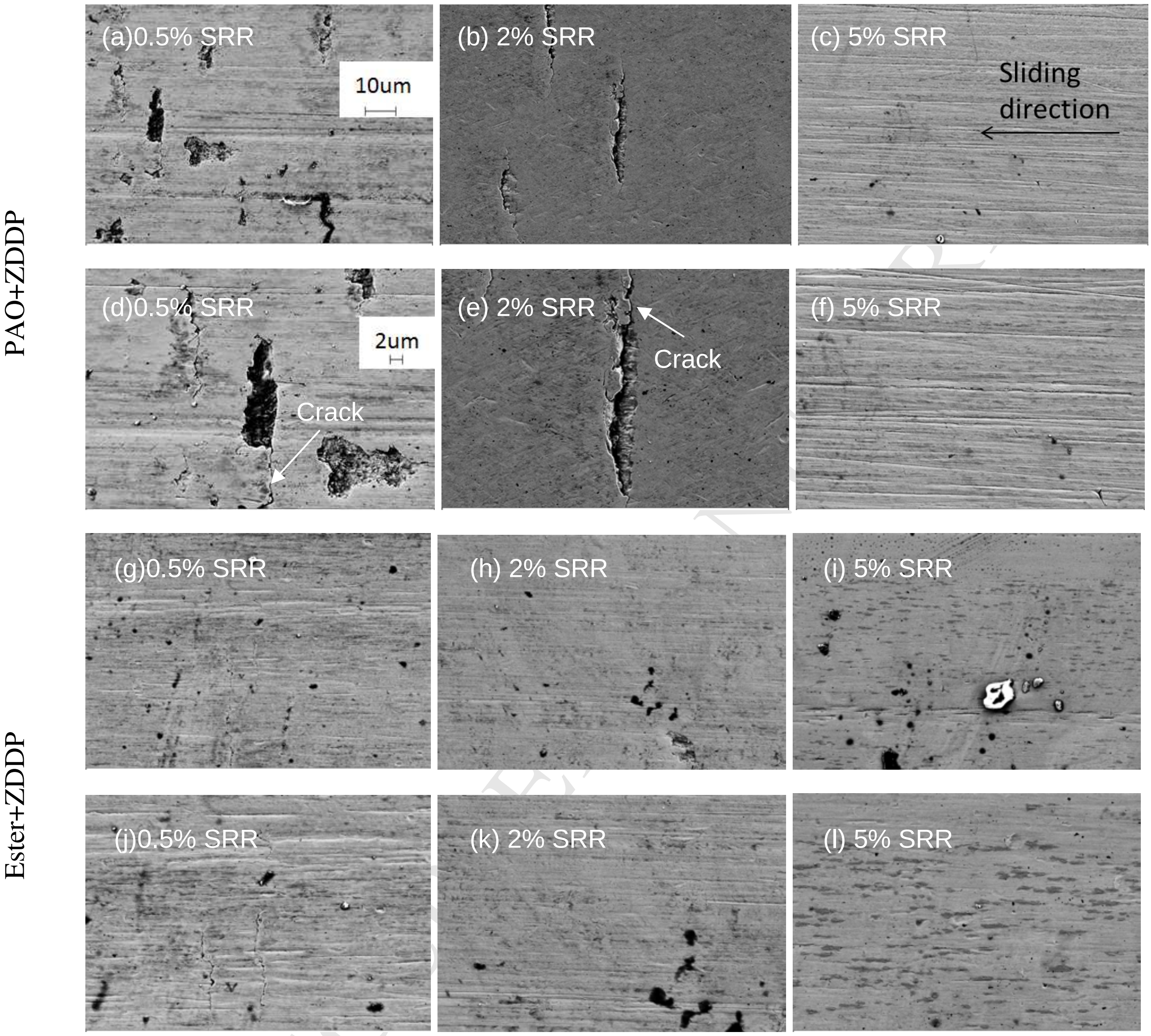

Fig. 5. SEM images of rollers after tribological tests:(a)-(f) are for PAO+ZDDP results; (g)-(l) are for Ester +ZDDP results; (a),(b),(c),(g),(h),(i)are in same scale as shown in (a); (d),(e),(f),(j),(k),(l) are in same scale as shown in (d).

The increase of SRR means more sliding occurs during the contact cycle. Therefore, the micropits formed on the surface can be more likely to be removed due to more sliding wear. In order to prove this, some shorter tests (5 mins, 30 mins, 60 mins) with PAO+ZDDP oils at 0.5%SRR and 5%SRR were done of which the wear results are shown in Fig. 6. Optical microscope images of rollers after shorter tribological tests are shown in Fig. 7 (all images are in the same scale as shown in Fig. 4). It can be concluded from Fig. 6 that the slope of

5%SRR is higher than 0.5%SRR, which means the wear rate (wear volume/time) at 5%SRR is higher than 0.5%SRR. Then, it is not surprising to see in Fig. 7 (d),(e),(f) that there is hardly any micropit formed on the roller surface at 5%SRR, while micropits could be seen at 0.5%SRR after 30 minutes and 60 minutes shown in Fig. 7 (b) and (c). This indicates that the formation process of micropits on the roller surface is directly related to wear. Moreover, the SEM images shown in Fig. 5 indicate that the micropits expand much faster at the direction perpendicular to the sliding direction than at the sliding direction. This is in line with the findings of Shotter [12] where he stated that the micropits propagate in the direction opposed to that of the traction force.

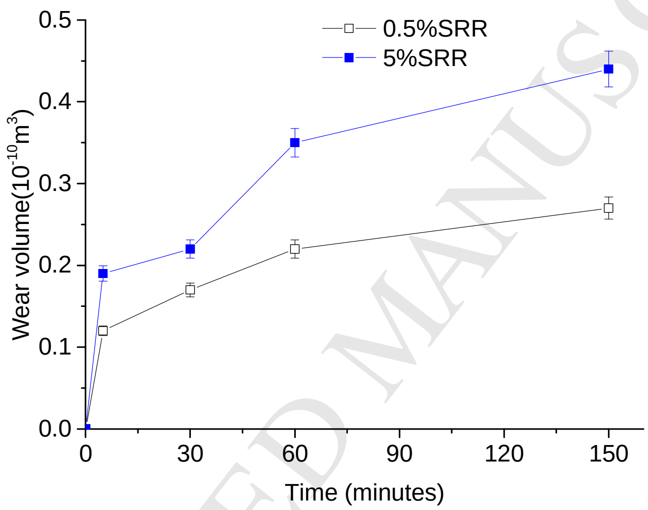

Fig. 6. Wear results of short tests with PAO+ZDDP oils under 0.5% and 5% SRR

The micropitting formation mechanism, explained by Oila and Bull [13] could be divided into initiation and propagation processes. Based on the findings in this research and explanations given in [13], the initiation and propagation process of micropits are illustrated in Fig. 8. The initiation process is shown in Fig. 8(a): within the rolling–sliding process, the asperity contacts of the rotating ring and roller generate alternating stresses which result in plastic deformation within the material beneath the asperity, then dislocation of the material caused by the asperity contact stress and deformation increases the hardness of the dislocated area. Therefore, the dark etching region (DER) forms where the hardness is lower than the dislocated area. As the cycling continues, the accumulation of the dislocations results in a slip band which initiates a crack and propagates along the boundary of DER because of the lower local hardness. The propagation process is shown in Fig. 8(b): the crack formed is preferable to propagate within the DER site. With the propagation of the crack and the combination effect of sliding, the dislocated material is removed and micropit is formed. Moreover, the propagation is also likely to occur within the white etching bands because of the existing spaces between them. Therefore, a complex network of cracks forms below the surface and results in wider and deeper micropits.

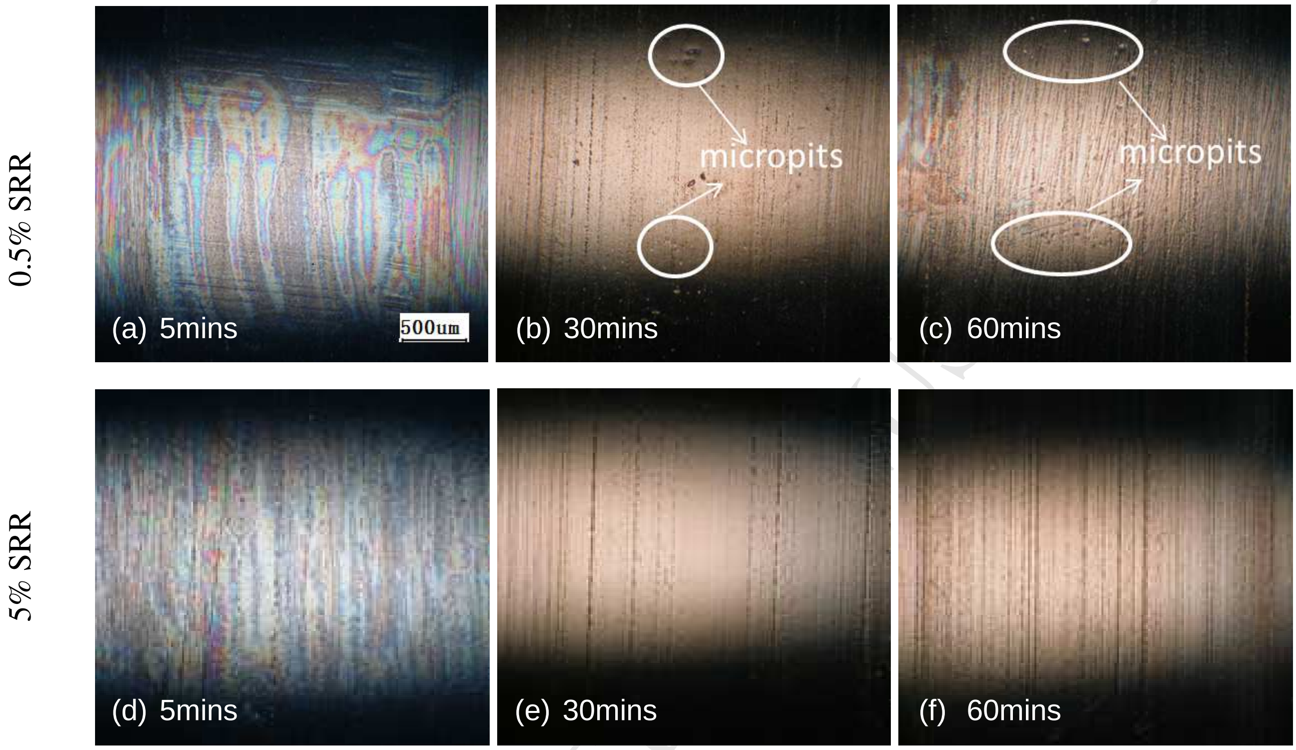

Fig. 7. Optical microscope images of rollers after short tribological tests with PAO+ZDDP oils: (a),(b),(c) are for 0.5%SRR results; (d),(e),(f) are for 5%SRR results; all figures are in same scale as shown in (a).

Shimizu et al.[14] applied Scanning Electron Microscopy with Energy Dispersive X-ray (SEM-EDX) and Atomic Force Microscope (AFM) technique to study the effect of SRR on ZDDP tribofilm. They found that SRR can affect the rubbing between the two contacting surfaces which then influence the ZDDP tribofilm formation process. In this paper, XPS is applied to study the tribofilm information under different SRRs.

3.2 Surface chemical properties

As only PAO+ZDDP oils have shown micropits formed on the roller after tribological tests, roller samples after 2.5 hours' tribological tests at 0.5%, 2% and 5% SRR with PAO+ZDDP was investigated by XPS to study the effect of SRR on the tribofilm. Fig. 9 shows the XPS element scan results of Fe 2p, Zn 2p and O 1s of post test roller at 0.5% SRR.

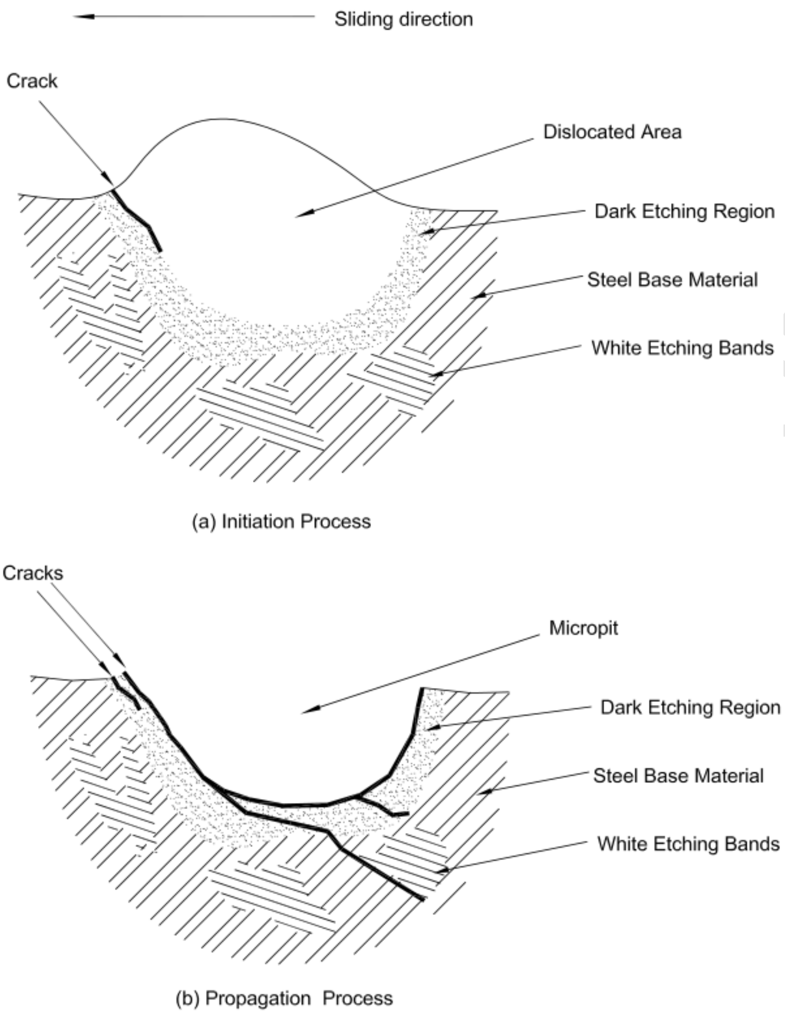

Fig. 8. Formation mechanism of micropit: (a) Initiation process; (b) Propagation Process [13]

It is shown in Fig. 9 (c) that the O 1s peak was curve fitted to bridging oxygen (BO) at 532.6±0.5 eV, non-bridging oxygen (NBO) 531.2±0.5 eV and oxide at 530.2±0.5 eV [14-15]. Bridging oxygen (BO) mainly contributes to the long chain compounds while non-bridging oxygen (NBO) mainly contributes to the short chain compounds. From previous published works [14-15], the type of metal oxide with the binding energies between 529.5-530.5 eV is iron oxide. Previous researches [16-18] have shown that ZDDP additive is effective in building up thick glassy Fe phosphate and Zn phosphate layers in the tribofilm. Nedelcu *et al.* [19] show that the chain length of phosphate is directly related to the wear performance of ZDDP-derived tribofilm.

Table 3 shows the element concentration Fe 2p, Zn 2p, P 2p, S 2p and O 1s as well as the binding energy of P $2p_{3/2}$ following the tests with PAO+ZDDP under different SRRs. The concentration of oxygen as oxide is observed to increase with SRR, which indicates more iron oxide forms in the tribofilm with the increase of SRR. The reason of increase wear of the contacting surfaces might be due to high hardness of the crystallised oxide and its relatively high melting point (>1200°C)[16]. But the hardness of this oxide is not actually known and will be tested by Nanoindentor in the future work. Furthermore, Spikes [20] and Gellman *et al.* [21] show that iron oxide is mostly found at the bottom layer of the ZDDP tribofilm. Thus, more iron oxide with the increase of SRR found in this study means more iron oxide with high hardness locates near to the substrate which increases the local hardness. Then, the cracks are less prone to propagate during the micopitting formation process (as shown in Fig. 8) and less micropits will form on the roller surface with the increase of SRR.

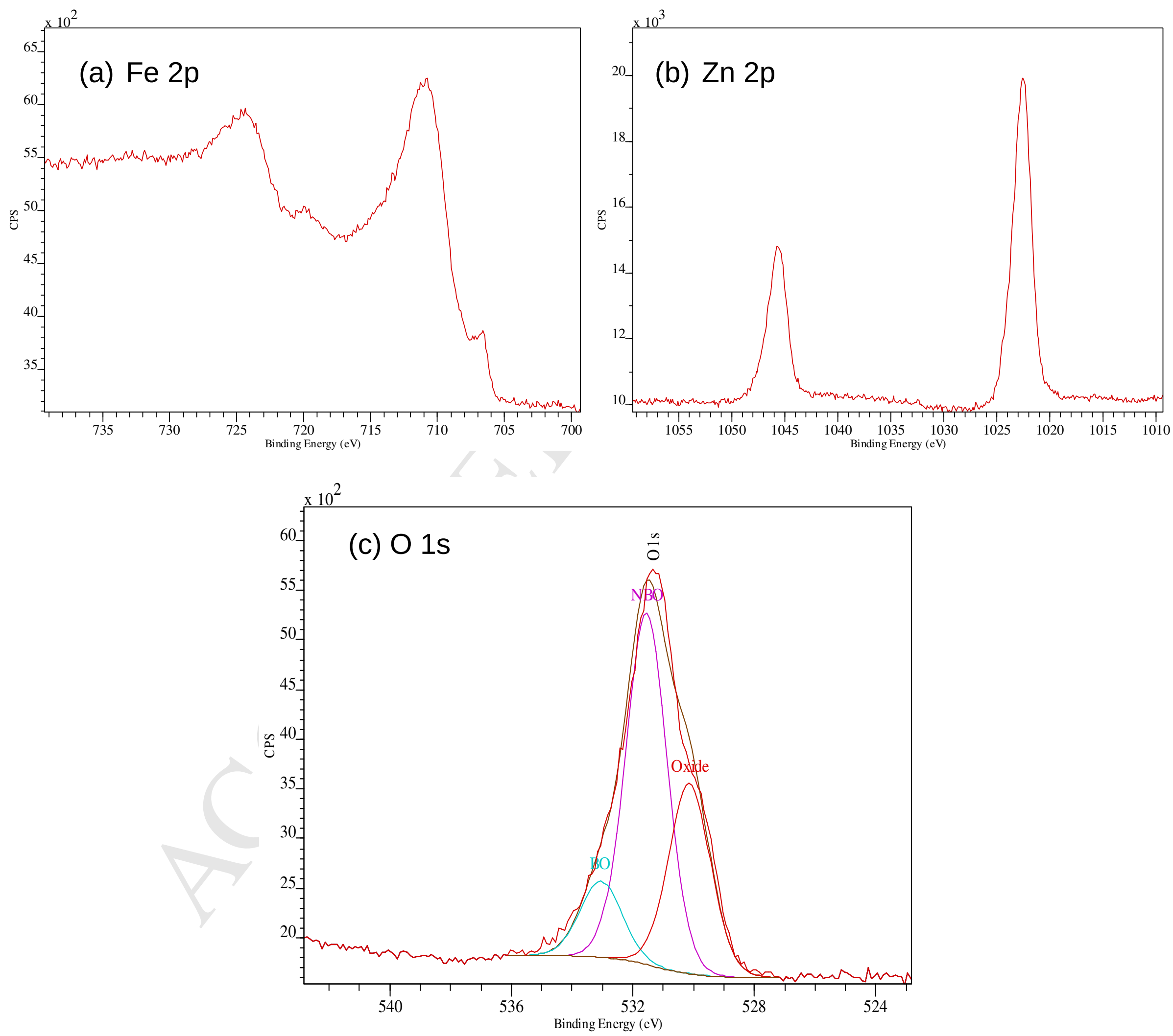

Fig. 9. XPS element scan results of post test roller at 0.5% SRR, following the test with PAO+ZDDP: (a) element scan results of Fe 2p; (b)element scan results of Zn 2p; (c)element scan results of O 1s.

Table 3 also shows the binding energy of P $2p_{3/2}$ under different SRRs. It is clear that the binding energy of P $2p_{3/2}$ did not change much with SRR considering the XPS testing accuracy is ±0.2 eV. However, the element concentration of BO increases while NBO decreases with SRR, which indicates phosphate chain length decreases with SRR. This is contradicting to the finding from Nedelcu *et al.* [19] where she believed that the phosphate chain length increases with SRR based on the increasing binding energy of P $2p_{3/2}$ with SRR. Moreover, the element concentration of P, S, Fe and Zn decreases with SRR shown in Table 3. Then it can be concluded that less ZDDP by products (Fe, Zn phosphate, sulphate, sulphide) remained on the roller surface with SRR. Therefore, it is not surprising to see the increasing wear with SRR.

Table 3 XPS scan results of post test rollers with PAO+ZDDP oils at different SRRs

SRR	Element concentration（%）							Position of P $2p_{3/2}$ (eV)
	Fe	Zn	P	S	BO	NBO	O（Oxide）	
0.5%	2.8	5.9	6.2	3.1	3.2	4.5	0.4	133.3
2%	1.9	1.9	4.1	1.7	1.5	4.6	0.6	133.4
5%	1.7	1.4	3.1	1.1	0.7	7.1	1.6	133.3

Another parameter which may affect the micropitting behaviour is layer thickness of the tribofilm. In this paper, XPS depth profiling acquisition (etching process) was used to study the changing trend of layer thickness with SRR. As mentioned by previous researches [21-23], iron oxide is at the bottom of the ZDDP tribofilm and just above the substrate. Therefore，Fe 2p and O 1s signals were selected to study the XPS depth profiling file. The etching process is terminated once the atomic concentration of O1s signal became lower than 5% when it is considered to reach the steel substrate [9,19]. Fig. 10 shows the XPS depth profiling file of Fe 2p and O 1s following tribological tests with PAO+ZDDP at different SRRs. It is obvious that it took less time of etching to obtain a steady iron and oxygen intensity from the roller substrate with the increase of SRR. This indicates that reaction layer (tribofilm) thickness decreases with SRR. With thinner tribofilm, the contacting surfaces are more prone to experience severe asperity contact. This might be another reason of the higher wear on the roller with the increase of SRR. With higher wear on the roller, the micropits formed will be more prone to be wiped off from the roller surface.

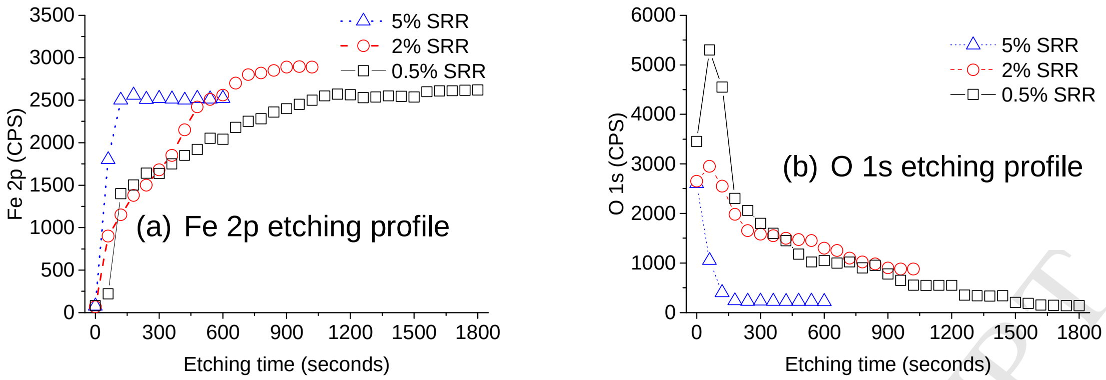

Fig. 10. XPS depth profiling file of Fe 2p and O 1s, following the test with PAO+ZDDP: (a) etching profile of Fe 2p; (b) etching profile of O 1s.

4 Conclusions

In this paper, the combined effect of SRR and lubricant chemistry on micropitting has been studied. The main conclusions are:

(1) The wear on roller increased with higher SRR, while friction did not change much.

(2) Less micropits formed on the roller surface with higher SRR. This can be related to higher wear as micropits can be wiped off from the roller surface due to wear.

(3) Micropitting formation and wear were affected by the polarity of base oil. Polar Ester oil can compete with ZDDP additive which results in higher wear and limits the effect of ZDDP in promoting the formation of micropits.

(4) The concentration of iron oxide was found to be higher in the tribofilm with higher SRR. This might be one possible reason of the higher wear and less micropits on the roller surface due to the high hardness of iron oxide, of which the hardness needs to be further studied in the future work.

(5) The film thickness on the roller surface decreased with higher SRR. This leads to more asperity contacts between the contacting surfaces which results in higher wear on the roller surface.

References

[1].Neville SS and AM and MCP van E and IN and A. Investigation of the effect of a diamine-based friction modifier on micropitting and the properties of tribofilms in rolling-sliding contacts. J Phys D Appl Phys 2016;49:505302.

[2].Rycerz P, Olver A, Kadiric A. Propagation of surface initiated rolling contact fatigue cracks in bearing steel. Int J Fatigue 2017;97:29–38. doi:https://doi.org/10.1016/j.ijfatigue.2016.12.004.

[3].Maya-Johnson S, Felipe Santa J, Toro A. Dry and lubricated wear of rail steel under rolling contact fatigue - Wear mechanisms and crack growth. Wear 2017;380–381:240–50. doi:https://doi.org/10.1016/j.wear.2017.03.025.

[4].Hutt S, Clarke A, Evans HP. Generation of Acoustic Emission from the running-in and subsequent micropitting of a mixed-elastohydrodynamic contact. Tribol Int 2018;119:270–80. doi:https://doi.org/10.1016/j.triboint.2017.11.011.

[5].Morales-Espejel GE, Rycerz P, Kadiric A. Prediction of micropitting damage in gear teeth contacts considering the concurrent effects of surface fatigue and mild wear. Wear 2018;398–399:99–115. doi:https://doi.org/10.1016/j.wear.2017.11.016.

[6].Lainé E, Olver A V, Beveridge TA. Effect of lubricants on micropitting and wear. Tribol Int 2008;41:1049–55. doi:https://doi.org/10.1016/j.triboint.2008.03.016.

[7].Lainé E, Olver A V, Lekstrom MF, Shollock BA, Beveridge TA, Hua DY. The Effect of a Friction Modifier Additive on Micropitting. Tribol Trans 2009;52:526–33. doi:10.1080/10402000902745507.

[8].Dowson D, Higginson GR. Elasto-hydrodynamic lubrication: the fundamentals of roller and gear lubrication. Pergamon Press 1966.

[9].Cen H, Morina A, Neville A, Pasaribu R, Nedelcu I. Effect of water on ZDDP anti-wear performance and related tribochemistry in lubricated steel/steel pure sliding contacts. Tribol Int 2012;56:47–57. doi:https://doi.org/10.1016/j.triboint.2012.06.011.

[10].Naveira Suarez A, Grahn M, Pasaribu R, Larsson R. The influence of base oil polarity on the tribological performance of zinc dialkyl dithiophospate additives. Tribol Int 2010;43:2268–78. doi:https://doi.org/10.1016/j.triboint.2010.07.016.

[11].Morales-Espejel GE, Brizmer V. Micropitting Modelling in Rolling–Sliding Contacts: Application to Rolling Bearings. Tribol Trans 2011;54:625–43. doi:10.1080/10402004.2011.587633.

[12].Shotter BA. Micropitting: Its characteristics and implications on the test requirements of gear oils. Performance and Testing of Gear Oils and Transmission Fluids, Institute of Petroleum. 1981:53-60.

[13].Oila A, Bull SJ. Assessment of the factors influencing micropitting in rolling/sliding contacts. Wear 2005;258:1510–24.

[14].Shimizu Y, Spikes HA. The Influence of Slide–Roll Ratio on ZDDP Tribofilm Formation. Tribol Lett 2016;64:19. doi:10.1007/s11249-016-0738-z.

[15].Nicholls MA, Do T, Norton PR, Kasrai M, Bancroft GM. Review of the lubrication of metallic surfaces by zinc dialkyl-dithiophosphates. Tribol Int 2005;38:15–39. doi:https://doi.org/10.1016/j.triboint.2004.05.009.

[16].Martin JM, Grossiord C, Le Mogne T, Bec S, Tonck A. The two-layer structure of Zndtp tribofilms: Part I: AES, XPS and XANES analyses. Tribol Int 2001;34:523–30. doi:https://doi.org/10.1016/S0301-679X(01)00029-9.

[17].Zhang J, Spikes H. On the Mechanism of ZDDP Antiwear Film Formation. Tribol Lett 2016;63:24. doi:10.1007/s11249-016-0706-7.

[18].Zhang J, Yamaguchi E, Spikes H. The Antagonism between Succinimide Dispersants and a Secondary Zinc Dialkyl Dithiophosphate. Tribol Trans 2014;57:57–65. doi:10.1080/10402004.2013.845275.

[19].Nedelcu I, Piras E, Rossi A, Pasaribu HR. XPS analysis on the influence of water on the evolution of zinc dialkyldithiophosphate–derived reaction layer in lubricated rolling contacts. Surf Interface Anal 2012;44:1219–24. doi:10.1002/sia.4853.

[20].Spikes H. The History and Mechanisms of ZDDP. Tribol Lett 2004;17:469–89. doi:10.1023/B:TRIL.0000044495.26882.b5.

[21].Gellman AJ, Spencer ND. Surface chemistry in tribology. Proc Inst Mech Eng Part J J Eng Tribol 2002;216:443–61. doi:10.1243/135065002762355352.

[22].Maboudian R, Carraro C. Surface Chemistry and Tribology of Mems. Annu Rev Phys Chem 2004;55:35–54. doi:10.1146/annurev.physchem.55.091602.094445.

[23].Feldman K, Fritz M, Hähner G, Marti A, Spencer ND. Surface forces, surface chemistry and tribology. Tribol Int 1998;31:99–105. doi:https://doi.org/10.1016/S0301-679X(98)00012-7.